International Journal of Engineering

Journal Homepage: www.ije.ir

Effect of Target Impedance Selection on the Lower Extremity Assistive Exoskeleton Performance

A. Taherifar[a], A. Selk Ghafari*[b], G. Vossoughi[a]

[a] School of Mechanical Engineering, Sharif University of Technology, Tehran, Iran
[b] School of Science and Engineering, Sharif University of Technology, International Campus, Kish Island, Iran

PAPER INFO

Paper history:
Received 09 December 2015
Received in revised form 31 January 2016
Accepted 02 June 2016

Keywords:
Lower Limb Exoskeleton
Impedance Control
Human-robot Modelling
Interaction Modelling

ABSTRACT

Exoskeletons are utilized extensively in robotic rehabilitation and power augmentation purposes. One of the most recognised control algorithms utilized in this field is the impedance controller. Impedance control approach provides the capability of realizing different rehabilitation exercises by tuning the target impedance gains. Trial and error experimental approach is one of the most common methods reported in the literature used to tune the target impedance. In this research, a general framework is proposed to study the effect of the target impedance selection on the exoskeleton performance and generation of the human gait profile. The dynamic model of the human-exoskeleton in the sagittal plane is derived for gait simulation study. In addition, a novel human-exoskeleton interaction model is introduced. The simulation study was carried out to illustrate that how the target impedance gains should be selected to minimize several criterias such as energy consumption, interaction forces and position tracking errors during walking. As a result, the proposed method provides better insight into the effective selection methods of the impedance control gains.

doi: *10.5829/idosi.ije.2016.29.06c.00*

1. INTRODUCTION

Exoskeletons are augmentation devices that provide the ability to carry heavy loads, increase the speed of movement and minimize the energy consumption during various activities. In addition, these robots served as assistive devices to restore the gait pattern for the disabled people and assist the elderly people to perform daily activities. The exoskeletons are mostly utilized for rehabilitation of the human with spinal cord injury (SCI) and stroke patients, muscle strengthen, resolving gait and balance disorders in old adults and treating the gait pathologies.

The most recently developed rehabilitation exoskeletons for patients with neurological disorders are LOKOMAT [1], LOPES [2] and Vanderbilt [3]. The therapeutic exercise devices are another kind of robots which deal with the patient with muscle disorder and after operation treatment [4, 5]. The main goal of these therapeutic exercises is to treat and resolve the effects of pain, spasm and edema, and return the injured patient to pain-free and fully functional activities [6]. A limited number of the rehabilitation exoskeletons have been clinically evaluated [1, 7], while the majority of the researches have been focused on experimental investigations on healthy people [8].

Since in the human-exoskeleton systems there are several complicated subsystems that must be carefully modelled, a few studies have focused on the complete modelling and simulation of the human and exoskeletons [9-13]. The human-robot system includes the robot dynamics and controller, human neuro-musculoskeletal system and the interaction model between them. The most challenging subsystem among them is the human neural model.

This paper presents the dynamic modelling of the human-exoskeleton walking issue in sagittal plane. One of the most recognised control methods utilized in human-robot corporation system is the impedance control. Mostly, the impedance gains called target impedance are adjusted experimentally with trial and error approach. To the best of our knowledge no research has been found on the effects of the target

*Corresponding Author's Email: *a_selkghafari@sharif.edu* (A. Selk Ghafari)

Please cite this article as: A. Taherifar, A. Selk Ghafari, G. Vossoughi, Effect of Target Impedance Selection on the Lower Extremity Assistive Exoskeleton Performance, International Journal of Engineering (IJE), TRANSACTIONS C: Aspects Vol. 29, No. 6, (June 2016)

impedance selection in presence of minimizing the specific cost function for the system under investigation. In this research, the integrated model of the human-exoskeleton is presented and the effects of target impedance of the robot on the required torque and energy consumption, position tracking error and interaction forces are analysed. We try to answer the following questions in this paper:

- Do the input torque and power of the human-exoskeleton change when the target impedance increases?
- How should the target impedance be changed to keep the interaction force minimum?
- Is it necessary to change the target impedance in the stance and swing phases during the movement?
- Does changing the target impedance, affect the tracking error of the human?
- How should the human model be changed to present the weak people characteristics?

2. Preliminary Gait Analysis

The clinical gait analysis (CGA) provides quantitative information to get better insight into understanding the ethology of the gait [14]. The human walking in CGA is normally divided into eight subsection called gait phases [15] as shown in the Figure 1. The walking starts with initial contact of the right leg and terminates with terminal swing.

Three phases namely, initial contact, loading response and pre swing are double support phases (DSP) and constrained dynamic equation must be used in these phases. Figure 2 presents the status of the virtual switches under the heel and the toe. In the Table 1, "*0*" stands for no contact and "*1*" stands for the foot contact with the ground. In DSP, the toe of the stance leg and the heel of the swing leg are always located in contact with the ground.

In the single support phase (SSP), the toe of the stance leg is always located in contact with the ground as indicated in Figure 2.

The heel of the stance leg is located in contact with the ground in the mid stance phase and rise slightly during the terminal stance. It should be noted that in this case, no limitative assumptions have been made in the gait modeling. In the next section the dynamic model of the SSP and DSP of a seven segment body will be presented.

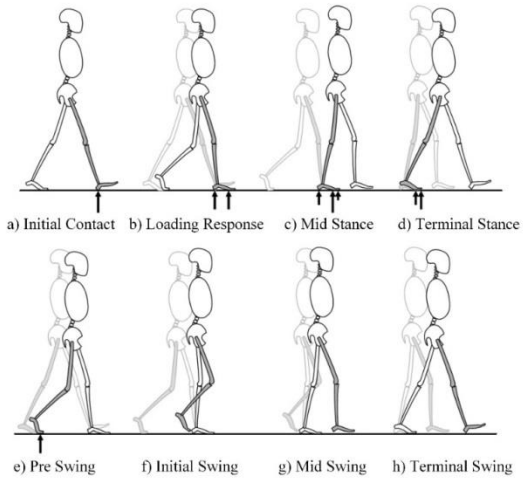

Figure 1. Fundamental gait phases in swing and stance phases

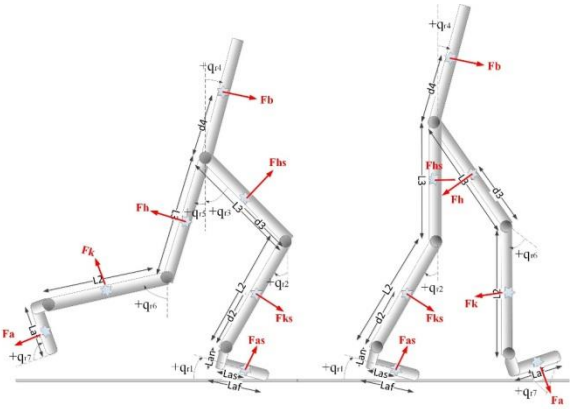

Figure 2. The seven segment dynamic model of the human-exoskeleton in a) single support phase and b) double support phase

TABLE 1. The status of the virtual switches under the heel and toe

Phases	Cycle	Left Heel	Left Toe	Right Heel	Right Toe	Stance Leg	Main Phase
Initial Contact	0	0	1	1	0	Left Leg	*DSP*
Load Responding	0 - 10%	0	1	1	1		*DSP*
Mid Stance	10% - 30%	0	0	1	1		SSP
Terminal Stance	30% - 50%	0	0	0	1	Right Leg	SSP
Pre Swing	50% - 60%	1	1	0	1		*DSP*
Initial Swing	60% - 73%	1	1	0	0		SSP
Mid Swing	73% - 87%	1	1	0	0	Left Leg	SSP
Terminal Swing	87% - 100%	0	1	1	0		SSP

3. DYNAMIC MODELLING OF HUMAN-EXOSKELETON

Based on the experimental investigation of human movement it is obvious that the most relevant torques and powers involved in human ambulation occur at the sagittal plane [16]. In this paper, a seven segment model limited to move in the sagittal plane is proposed to model human-exoskeleton motion as depicted in Figure 2. The human and exoskeleton limbs are connected to each other by straps at the points shown by star in each link. The direction of the interaction forces between the human and exoskeleton is assumed to be perpendicular to the limbs as shown in this figure. In SSP, the toe of the stance leg is hinged to the ground and the remaining bodies are connected serially as a 7-DOF system. In DSP, the toe of the stance leg is again hinged to the ground and the heel of the swing leg is kinematically constrained to be in contact with ground as a 5-DOF system.

Referring to the data given in Table 1, it is assumed that in phase a and b, the left leg is the stance leg and the body is located in double support phase. Furthermore, phase c and d are single supported and the right leg is the stance leg. The phase c is double supported and again the right leg is the stance leg. Finally the phase f, g and h are single supported and the left leg is the stance leg.

3. 1. Single Support Phase Model The SSP dynamic model of the human-exoskeleton illustrated in Figure 2 has 7-degrees-of-freedom. The absolute angle of the limbs in clockwise sense $q=[q_1,q_2,\cdots,q_7]$, are defined and considered as the generalised coordinates. The dynamic model of the human-exoskeleton are derived utilizing Lagrange approach as follows:

$$\begin{aligned} &\boldsymbol{M}_r(\boldsymbol{q}_r)\ddot{\boldsymbol{q}}_r+\boldsymbol{v}_r(\boldsymbol{q}_r,\dot{\boldsymbol{q}}_r)+\boldsymbol{g}_r(\boldsymbol{q}_r)=\boldsymbol{B}_r\boldsymbol{\tau}_r-\boldsymbol{J}^T\boldsymbol{f}_{int}\\ &\boldsymbol{M}_h(\boldsymbol{q}_h)\ddot{\boldsymbol{q}}_h+\boldsymbol{v}_h(\boldsymbol{q}_h,\dot{\boldsymbol{q}}_h)+\boldsymbol{g}_h(\boldsymbol{q}_h)=\boldsymbol{B}_r\boldsymbol{\tau}_h+\boldsymbol{J}^T\boldsymbol{f}_{int}\end{aligned} \quad (1)$$

where r and h subscripts stand for the exoskeleton and human, respectively. $\boldsymbol{q}$ is the generalised coordinates, $\boldsymbol{M(q)}$ is a 7×7 symmetric positive definite inertia matrix, $\boldsymbol{V(q,\dot{q})}$ is 7×1 centrifugal and Coriolis vector, $\boldsymbol{g(q)}$ is 7×1 vector containing the gravity effects, $\boldsymbol{\tau}$ is the joint torque, $\boldsymbol{B}$ maps the joint torques to the limbs torques, $\boldsymbol{f}_{int}$ is the interaction force exerted by human to the exoskeleton in star points (refer to the Figure 2) and J is the Jacobian matrix defined as,

$$\boldsymbol{v}=\boldsymbol{J}\dot{\boldsymbol{q}}_r \quad (2)$$

where $\boldsymbol{v}$ is the linear velocity of the interaction points. The dynamic model is validated by Simmechanics toolbox of MATLAB software. The relative error was set less than 10^{-3} N.m in inverse dynamic simulation.

3. 2. Double Support Phase Model The dynamic model in DSP is the same as SSP model except that two constraint equations must be satisfied. The heel of the swing leg position in horizontal and vertical directions must be kept constant during this phase. Constraints reduce the degree of freedom of the model to five. In this case, the governing dynamic equations of DSP are formulate as follows,

$$\begin{aligned} &\boldsymbol{M}_r(\boldsymbol{q}_r)_{7\times7}\ddot{\boldsymbol{q}}_r+\boldsymbol{v}_r(\boldsymbol{q}_r,\dot{\boldsymbol{q}}_r)_{7\times1}+\boldsymbol{g}_r(\boldsymbol{q}_r)_{7\times1}=\\ &\boldsymbol{B}_{r\,7\times7}\boldsymbol{\tau}_{r\,7\times1}-\boldsymbol{J}^T{}_{7\times7}\boldsymbol{f}_{int\,7\times1}+\boldsymbol{J}_{DSP\,7\times2}\boldsymbol{R}_{2\times1}\end{aligned} \quad (3)$$

where $\boldsymbol{R}$ is the reaction force at the heel of the swing leg and J_{DSP} is the Jacobian matrix which maps the reaction force moment to the joint space. Equation (3) is multiplied by the null space of $\boldsymbol{J}_{DSP}$ from right hand side to eliminate the last term of the equation as follows,

$$\begin{aligned} &\underbrace{\times\left(\boldsymbol{NullJ}_{DSP}\right)^T_{2\times7}}\bar{\boldsymbol{M}}_r(\boldsymbol{q}_r)_{5\times7}\ddot{\boldsymbol{q}}_r+\bar{\boldsymbol{v}}_r(\boldsymbol{q}_r,\dot{\boldsymbol{q}}_r)_{5\times1}\\ &+\bar{\boldsymbol{g}}_r(\boldsymbol{q}_r)_{5\times1}=\bar{\boldsymbol{B}}_{r\,5\times7}\boldsymbol{\tau}_{r\,7\times1}-\bar{\boldsymbol{J}}^T_{5\times7}\boldsymbol{f}_{int\,7\times1}\end{aligned} \quad (4)$$

Since two constraints are satisfied, Equation (5) presents 5 independent equations. Similar formulation can be derived to present human dynamics in DSP.

4. HUMAN INTERACTION MODELLING

The exoskeleton limbs are connected to the human limb employing straps. In this case, exoskeleton and human limbs move with different angles during motion. Most of the models presented in the literature assume the same limb's angles for human and exoskeleton limbs during the movement. Since the straps used to connect the exoskeleton and human limbs mainly have high stiffness and damping properties [17], the following interaction model can be considered:

$$\begin{aligned}\boldsymbol{f}_{int}&=\boldsymbol{K}_s\Delta\boldsymbol{x}+\boldsymbol{C}_s\Delta\dot{\boldsymbol{x}}=\boldsymbol{K}_s\boldsymbol{J}\Delta\boldsymbol{q}+\boldsymbol{C}_s\boldsymbol{J}\Delta\dot{\boldsymbol{q}}\\&=\boldsymbol{K}_s\boldsymbol{J}(\boldsymbol{q}_h-\boldsymbol{q}_r)+\boldsymbol{C}_s\boldsymbol{J}(\dot{\boldsymbol{q}}_h-\dot{\boldsymbol{q}}_r)\end{aligned} \quad (5)$$

where $\boldsymbol{K}_s$ and $\boldsymbol{C}_s$ are the spring and damping constants of the straps.

5. IMPEDANCE CONTROL

Impedance control introduced by Hogan [18] is the most recognised controller in human-exoskeleton interaction. In the impedance control, a mass-spring-damper relation is defined and the controller attempts to correlate the position tracking error to the interaction force according to this relation.

There are two common approaches used to implement impedance control [19, 20], known as position based and torque based approaches. Here, the torque based approach (feedback linearized inner loop) is considered. If the desired position of the generalised coordinates defined as q_d, the feedback control law can be formulate as follows:

$$\begin{aligned}&\tilde{q} = q_d - q_r\\&\tau_r = B_r^{-1}\left(M_r(q_r)\zeta + v_r(q_r,\dot{q}_r) + g_r(q_r) + J^T f_{int}\right)\\&\zeta = \ddot{q}_d + M_{dr}^{-1}\left(K_{dr}\tilde{q} + C_{dr}\dot{\tilde{q}} + J^T f_{int}\right)\end{aligned} \quad (6)$$

where $\tilde{q}$ is the position tracking error, K_{dr}, C_{dr} and M_{dr} are the stiffness, damping and inertia target impedance matrices of the exoskeleton, respectively. It is assumed that the target impedance matrices are 7×7 diagonal. Doing some simplification and substitution in Equation (6), the control law can be found and presented as follows:

$$\begin{aligned}&\tau_r = B_r^{-1}\left(M_r(q_r)\left(\ddot{q}_d + M_{dr}^{-1}\left(K_{dr}\tilde{q} + C_{dr}\dot{\tilde{q}} + J^T f_{int}\right)\right)\right.\\&\left. + B_r^{-1}\left(v_r(q_r,\dot{q}_r) + g_r(q_r) + J^T f_{int}\right)\right.\end{aligned} \quad (7)$$

where f_{int} is calculated from Equation (5). Substituting Equation (7) into the exoskeleton dynamic Equation (1), the following desired impedance relation is obtained and given by,

$$M_{dr}\ddot{\tilde{q}} + C_{dr}\dot{\tilde{q}} + K_{dr}\tilde{q} = -J^T f_{int} \quad (8)$$

Equation (8) presents a compliant relation between the interaction force and position tracking error of the exoskeleton. The same controller can be used in DSP, except that pseudo inverse of B_r which must be employed instead of B_r^{-1}. So far, the integrated dynamic model of the human skeletal and exoskeleton structure is derived and the impedance controller is developed for the exoskeleton.

For the paralysed human one can consider the passive torque of the muscles and simulate the human-exoskeleton model using Equation (1) and (7). Furthermore, for a able bodied, weak or partially paralysed human the central nervous system (CNS) of the human must be modelled and simulated. Since the neural system of the human is too complicated, the most acceptable controller for the human neural system used in gait is utilized in this research. Referring to the results presented in the literature, human use antagonist coactivation of the muscles to realize the variable impedance control during motion [10, 18]. In this research, we assume that human utilize the impedance controller presented by Equation (7) (the sign of $J^T f_{int}$ will change to negative) to cancel its own inertia and gravitational terms (feed-forward) to produce the target impedance (position feedback).

$$M_{dh}\ddot{\tilde{q}}' + C_{dh}\dot{\tilde{q}}' + K_{dh}\tilde{q}' = J^T f_{int} \quad (9)$$

where $\tilde{q}' = q_d - q_h$ is the human position tracking error, q_d is the same as the desired trajectory of the robot, K_{dh}, C_{dh} and M_{dh} are the stiffness, damping and inertia target impedance matrices, respectively.

Figure 3 shows the schematic of the integrated human-exoskeleton model for each limb. The desired impedance gains of human are K_{dh}, C_{dh}, M_{dh} and the desired impedance gains of the exoskeleton are K_{dr}, C_{dr}, M_{dr}. A few works has been done to answer the question of how these target impedance matrices should be modulated [9, 21, 22]. In the simulation section of this paper, the selection of the target impedance for a healthy and weak person will be discussed extensively.

Several approaches can be used to model the weakness of the human. Here, the weakness is considered as a general term related to any type of disability, which are listed as follows:

1. Since the control strategy employed by human is impedance control, one can realize that the weakness of the human can be presented by saturation of the human's joint torque (τ_h). It means that human neural system is performing perfect but the muscles cannot generate required force or torques.

2. The desired trajectory (q_d) of the impedance control might be abnormal due to spinal cord injuries. The desired trajectory of a healthy people can be scaled down to actualise the neurological problems during the gait.

3. The target impedance of the human (K_{dh}, C_{dh}, M_{dh}) can be reduced to decrease the joint torque and the muscles force consequently, when the patient has painful muscles or tendons. Also the target impedance can be increased for rough modelling of the spasticity.

4. In the case where the patient has weak muscles or painful joints, the patient cannot tolerate its own weight, therefore a proportion of centrifugal and gravitational terms ($v_h(q_h,\dot{q}_h) + g_h(q_h)$) must be considered in the human control law instead of the complete terms.

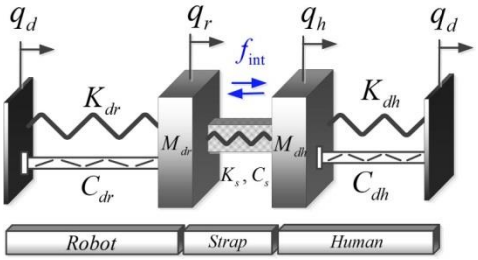

Figure 3. Human-exoskeleton interaction model for each limb. The exoskeleton and human use impedance control and the interaction is considered as spring-damper relation.

6. STABILITY ANALYSIS

The stability of the integrated human-exoskeleton system is proved by defining a positive definite Lyapunov function as:

$$V = \frac{1}{2}\dot{\tilde{\boldsymbol{q}}}^T \boldsymbol{M}_{dr}\dot{\tilde{\boldsymbol{q}}} + \frac{1}{2}\tilde{\boldsymbol{q}}^T \boldsymbol{K}_{dr}\tilde{\boldsymbol{q}} + \frac{1}{2}\dot{\tilde{\boldsymbol{q}}}'^T \boldsymbol{M}_{dh}\dot{\tilde{\boldsymbol{q}}}' + \frac{1}{2}\tilde{\boldsymbol{q}}'^T \boldsymbol{K}_{dh}\tilde{\boldsymbol{q}}' + \frac{1}{2}(\boldsymbol{q}_r - \boldsymbol{q}_h)^T \boldsymbol{K}_s(\boldsymbol{q}_r - \boldsymbol{q}_h) \quad (10)$$

where $\tilde{\boldsymbol{q}}$ and $\tilde{\boldsymbol{q}}'$ are the same as defined previously. Taking the derivative of the Lyapunov function yields:

$$\dot{V} = \dot{\tilde{\boldsymbol{q}}}^T \boldsymbol{M}_{dr}\ddot{\tilde{\boldsymbol{q}}} + \dot{\tilde{\boldsymbol{q}}}^T \boldsymbol{K}_{dr}\tilde{\boldsymbol{q}} + \dot{\tilde{\boldsymbol{q}}}'^T \boldsymbol{M}_{dh}\ddot{\tilde{\boldsymbol{q}}}' + \dot{\tilde{\boldsymbol{q}}}'^T \boldsymbol{K}_{dh}\tilde{\boldsymbol{q}}' + (\dot{\boldsymbol{q}}_r^T - \dot{\boldsymbol{q}}_h^T)\boldsymbol{K}_s(\boldsymbol{q}_r - \boldsymbol{q}_h) \quad (11)$$

Substituting $\ddot{\tilde{\boldsymbol{q}}}$ and $\ddot{\tilde{\boldsymbol{q}}}'$ from Equations (8) and (9), respectively yields:

$$\dot{V} = \dot{\tilde{\boldsymbol{q}}}^T(\boldsymbol{J}^T \boldsymbol{f}_{int} - \boldsymbol{C}_{dr}\dot{\tilde{\boldsymbol{q}}} - \boldsymbol{K}_{dr}\tilde{\boldsymbol{q}}) + \dot{\tilde{\boldsymbol{q}}}^T \boldsymbol{K}_{dr}\tilde{\boldsymbol{q}} + \dot{\tilde{\boldsymbol{q}}}'^T(-\boldsymbol{J}^T \boldsymbol{f}_{int} - \boldsymbol{C}_{dh}\dot{\tilde{\boldsymbol{q}}}' - \boldsymbol{K}_{dh}\tilde{\boldsymbol{q}}') + \dot{\tilde{\boldsymbol{q}}}'^T \boldsymbol{K}_{dh}\tilde{\boldsymbol{q}}' + (\dot{\boldsymbol{q}}_r - \dot{\boldsymbol{q}}_h)^T \boldsymbol{K}_s(\boldsymbol{q}_r - \boldsymbol{q}_h) \quad (12)$$

Performing some simplification, $\dot{V}$ expressed as follows,

$$\dot{V} = -(\boldsymbol{q}_r^T - \boldsymbol{q}_h^T)\boldsymbol{J}^T \boldsymbol{f}_{int} - \dot{\tilde{\boldsymbol{q}}}^T \boldsymbol{C}_{dr}\dot{\tilde{\boldsymbol{q}}} - \dot{\tilde{\boldsymbol{q}}}'^T \boldsymbol{C}_{dh}\dot{\tilde{\boldsymbol{q}}}' + (\dot{\boldsymbol{q}}_r - \dot{\boldsymbol{q}}_h)^T \boldsymbol{K}_s(\boldsymbol{q}_r - \boldsymbol{q}_h) \quad (13)$$

Substituting $\boldsymbol{f}_{int}$ from Equation (5) and applying $\dot{\boldsymbol{q}}_r - \dot{\boldsymbol{q}}_h = \dot{\tilde{\boldsymbol{q}}}' - \dot{\tilde{\boldsymbol{q}}}$ gives,

$$\dot{V} = -(\dot{\tilde{\boldsymbol{q}}}'^T - \dot{\tilde{\boldsymbol{q}}}^T)\boldsymbol{J}^T \boldsymbol{C}_s \boldsymbol{J}(\dot{\tilde{\boldsymbol{q}}}' - \dot{\tilde{\boldsymbol{q}}}) - \dot{\tilde{\boldsymbol{q}}}^T \boldsymbol{C}_{dr}\dot{\tilde{\boldsymbol{q}}} - \dot{\tilde{\boldsymbol{q}}}'^T \boldsymbol{C}_{dh}\dot{\tilde{\boldsymbol{q}}}' \quad (14)$$

It can be inferred that the derivative of the Lyapunov function is consist of a dissipative energy due to damping in human, exoskeleton and straps. Note that $\boldsymbol{C}_{dh}$ and $\boldsymbol{C}_s$ are positive definite. Therefore, supposing,

$\left\|\dot{\tilde{\boldsymbol{q}}}\right\|^2 \le \alpha$, $\left\|\dot{\tilde{\boldsymbol{q}}}'\right\|^2 \le \beta$, $\left\|\boldsymbol{J}(\dot{\tilde{\boldsymbol{q}}}' - \dot{\tilde{\boldsymbol{q}}})\right\|^2 \le \gamma$

One can infer that,

$$\dot{V} \le -\lambda_{\min}(\boldsymbol{C}_s)\gamma - \lambda_{\min}(\boldsymbol{C}_{dr})\alpha - \lambda_{\min}(\boldsymbol{C}_{dh})\beta \quad (15)$$

The human-exoskeleton system is locally marginally stable ($\dot{V} \le 0$) if,

$$\lambda_{\min}(\boldsymbol{C}_{dr}) \ge -\frac{\lambda_{\min}(\boldsymbol{C}_s)\gamma + \lambda_{\min}(\boldsymbol{C}_{dh})\beta}{\alpha} = -\boldsymbol{C}_{critical} \quad (16)$$

It means that in the case where $\boldsymbol{C}_{dr}$ is a diagonal matrix, the element of $\boldsymbol{C}_{dr}$ must be bigger than $-\boldsymbol{C}_{critical}$ to have a stable system.

7. IMULATION RESULTS

The simulation results of the integrated human-exoskeleton model during normal gait are presented in this section. The anthropometric parameters of the able bodied human are used for simulation study and given in Table 2 [23]. The desired trajectory of the links ($\boldsymbol{q}_d$) are also adopted from normal gait of a healthy human [23].

In the first part of the simulation, the effect of the human target impedance is investigated, merely. On the other hand, there is no interaction between the human and the exoskeleton.

The target impedance of the human is varied according to the data presented in Table 3. It is assumed that the impedance matrices are diagonal with identical elements. The target inertia matrix is assumed to be constant since it varies slightly. The Root Mean Square (RMS) of the energy consumption of the human during the stance and swing phases is determined based on Equation (1) and shown in Figure 4(a-b). It can be observed that the energy consumption during the stance phase is much more than the swing phase due to high weight bearing. The RMS of the torque and position tracking error of the knee joint are indicated in Figure 4 (c-f). Note that the torque of the ankle and hip joints have the same trend as the knee joint, which are not shown here. The torque of the knee joint and the energy consumption of the whole system will rise when $\boldsymbol{K}_{dh}$ is increased. The rate of the increment is greater in low target damping. The minimum energy and torque of the human in stance phase occurred at $\boldsymbol{K}_{dh}$=80N.m, while there is no significant amount of change in the knee joint torque during the swing phase.

TABLE 2. Physical properties of a normal human with 56.7 Kg weight and 1.7 m height [23]

Segment/ Parameter	Length (m)	Mass (Kg)	Moment of Inertia (Kg.m^2)	Center of Mass – Distal (m)
Foot	0.208	0.822	8.153e-4	0.104
Shank	0.418	2.637	0.042	0.209
Thigh	0.417	5.67	0.102	0.208
Trunk	0.799	38.95	6.118	0.4

TABLE 3. Human target impedance variation in the first part of the simulation

M_{dh} (Kg.m^2)	C_{dh} (N.s/m) Low damping	Medium damping	High damping	K_{dh} (N.m)
0.01	2-3	4-6	7-10	1-200

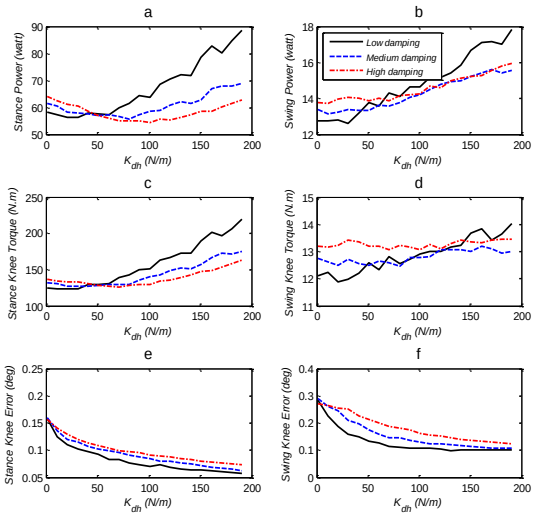

Figure 4. RMS of energy consumption of the human during the a) stance and b) swing phases. RMS of human knee torque during the c) stance and d) swing phases. RMS of knee position tracking error for e) stance and f) swing phases.

Unlike the joint torque, the position tracking error will decrease by stiffing the target impedance of the human; moreover, the position error sensitivity to the target impedance variation during the swing phase is more than stance phase.

It can be concluded that, human tends to decrease the stiffness and damping in swing joint to decrease the energy consumption and torque. On the other hand, decreasing the stiffness and damping result in higher position tracking error. Since the stability of the gait is mainly adjusted by trunk, the positioning error of the swing phase does not significantly affect the stability. So, $\boldsymbol{K_{dh}}$ and $\boldsymbol{C_{dh}}$ are set to 10N.m and 2N.s/m, respectively, for a healthy person in the swing phase.

On the other hand, the human tends to consume minimum energy while avoids high position tracking error to keep balance during the stance phase. As a result, for a healthy person during the stance phase, $\boldsymbol{K_{dh}}$ and $\boldsymbol{C_{dh}}$ are set to 80N.m and 7 N.s/m, respectively.

In the second part of the simulation study, the target impedance of the exoskeleton is varied while the target impedance of the human is kept constant. The strap stiffness ($\boldsymbol{K}_s$) and damping ($\boldsymbol{C}_s$) are assumed to be 20000 N/m and 500 N.s/m, respectively. As discussed in section 5, there are four ways to model the human weakness. Here, it is assumed that the human strength is such that it cannot tolerate more than 70% of its own weight (fourth case). Also, the desired impedances are selected 5N.m, 0.5 N.s/m and 0.01 Kg.m^2 due to painful muscles and joints (third case).

Figure 6 shows the RMS torque of the ankle, knee and hip joints for the exoskeleton and human during the stance and swing phases. Since the joints of the stance leg endure the most of the weight, they employ much more torque than swing joints in human and the robot. Furthermore, since 70% of the human weight is tolerated by itself, the human joints provide torques more than the exoskeleton's. In addition, the ankle joint during stance phase delivers the largest torque which confirms the CGA results [23].

Simulation results presented in Figure 6 indicate that high stiffness and low damping during stance phase brings the human and exoskeleton to the margin of instability and demands relatively high torque. Referring to the results presented in Figure 6 (e, d and f), it can be observed that high damping will greatly reduce the human joint torques in ankle, knee and hip joints while the RMS torque of the exoskeleton will increase to assist the patient in this phase (Figure 6 (b, d, f)).

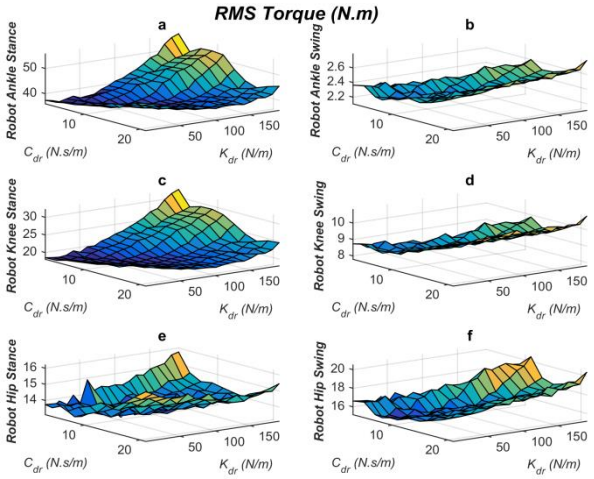

Figure 5. The RMS of joint torques (N.m) of a) exoskeleton's ankle in stance, b) exoskeleton's ankle in swing, c) exoskeleton's knee in stance, d) exoskeleton's knee in swing, e) exoskeleton's hip in stance, f) exoskeleton's hip in swing.

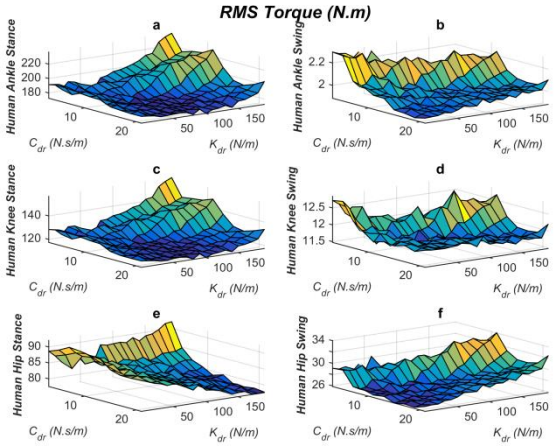

Figure 6. The RMS of joint torques (N.m) of a) human ankle in stance, b) human ankle in swing, c) human knee in stance, d) human knee in swing, e) human hip in stance and f) human hip in swing phase.

Figure 7 indicates the RMS input power of the human and exoskeleton in stance and swing phases. Refer to the simulation results illustrated in this figure, it can be observed that increasing the impedance of the exoskeleton can highly reduce the input power of the human during the stance phase. In other words, the exoskeleton provides assisting of the weak patient in this phase without significant changes in the energy consumption of the human during the swing phase.

Figure 8 shows the interaction force and power in stance and swing phases. The minimum interaction force between the human and exoskeleton indicates the minimum assistance of the exoskeleton which occurs at the lowest impedance of the robot.

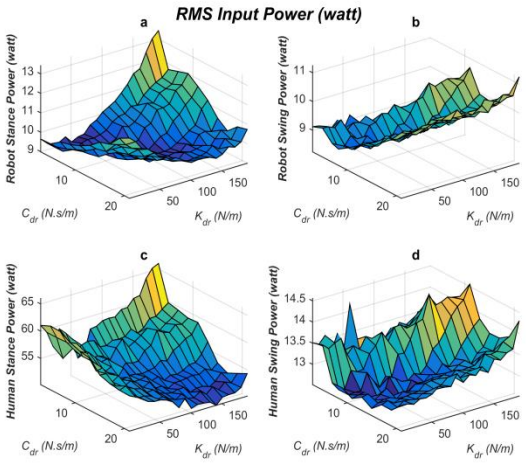

Figure 7. The RMS of the input power for a) exoskeleton in stance, b) exoskeleton in swing, c) human in stance and d) human in swing phase

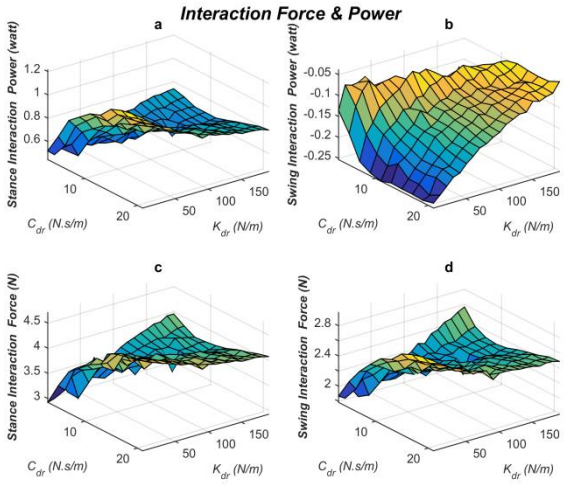

Figure 8. The average of interaction power (watt) in a) stance and b) swing phase. The average of interaction force (N) in c) stance and d) swing phase

On the other hand, the maximum interaction force means the maximum assistance of the exoskeleton which occurs at high damping and low stiffness of the assistive device. As a result, the target impedance of the exoskeleton's joint can be adjusted separately for a patient with certain weakness according to various criterion such as energy analysis, input torque or power and interaction force between the exoskeleton and human.

8. CONCLUSION

Impedance control is one of the most practical controllers used in human-exoskeleton interaction systems and especially in robotic rehabilitation. The target impedance determines the performance of the controller in terms of tracking, interaction force and energy consumption. This paper studies the appropriate selection procedure for the impedance gains of an exoskeleton cooperating with a weak patient during the gait. For this purpose, the dynamic model of the human-exoskeleton is derived and the impedance controller is proposed to control the system during gait generation. In the proposed model, deviation between the joint angle of the human and exoskeleton joints are considered. The impedance gains are selected by minimizing several criteria such as energy consumption of the human or exoskeleton, interaction force and position tracking error during complete gait cycle. Simulation study illustrates the effectiveness of the proposed framework for target impedance adjustment in comparison to the conventional trial and error approach utilized in the previous researches.

9. REFERENCES

1. Colombo, G., Joerg, M., Schreier, R. and Dietz, V., "Treadmill training of paraplegic patients using a robotic orthosis", ***Journal of Rehabilitation Research & Development***, Vol. 37, No. 6, (2000).
2. Veneman, J.F., Kruidhof, R., Hekman, E.E., Ekkelenkamp, R., Van Asseldonk, E.H. and Van Der Kooij, H., "Design and evaluation of the lopes exoskeleton robot for interactive gait rehabilitation", ***Neural Systems and Rehabilitation Engineering, IEEE Transactions on***, Vol. 15, No. 3, (2007), 379-386.
3. Farris, R.J., Quintero, H.A. and Goldfarb, M., "Preliminary evaluation of a powered lower limb orthosis to aid walking in paraplegic individuals", ***Neural Systems and Rehabilitation Engineering, IEEE Transactions on***, Vol. 19, No. 6, (2011), 652-659.
4. Sakaki, T., Okada, S., Okajima, Y., Tanaka, N., Kimura, A., Uchida, S., Taki, M., Tomita, Y. and Horiuchi, T., "Tem: Therapeutic exercise machine for hip and knee joints of spastic patients", in Proceeding of Sixth International Conference on Rehabilitation Robotics., (1999), 183-186.

5. Akdogan, E., Tacgın, E. and Adli, M.A., "Knee rehabilitation using an intelligent robotic system", ***Journal of Intelligent Manufacturing***, Vol. 20, No. 2, (2009), 195-202.
6. Akdogan, E. and Adli, M.A., "The design and control of a therapeutic exercise robot for lower limb rehabilitation: Physiotherabot", ***Mechatronics***, Vol. 21, No. 3, (2011), 509-522.
7. Koopman, B., Van Asseldonk, E.H. and Van der Kooij, H., "Selective control of gait subtasks in robotic gait training: Foot clearance support in stroke survivors with a powered exoskeleton", ***Journal of NeuroEngineering and Rehabilitation***, Vol. 10, No. 1, (2013), 3-12.
8. Taherifar, A., Mousavi, M., Rassaf, A., Ghiasi, F. and Hadian, M., "Lokoiran—a novel robot for rehabilitation of spinal cord injury sand stroke patients", in Proceedings of the RSI/ISM International Conference on Robotics and Mechatronics., (2013).
9. Emken, J.L., Benitez, R., Sideris, A., Bobrow, J.E. and Reinkensmeyer, D.J., "Motor adaptation as a greedy optimization of error and effort", ***Journal of Neurophysiology***, Vol. 97, No. 6, (2007), 3997-4006.
10. Osu, R., Morishige, K.-i., Miyamoto, H. and Kawato, M., "Feedforward impedance control efficiently reduce motor variability", ***Neuroscience Research***, Vol. 65, (2009), 6-10.
11. Garmsiri, N., Najafi, F. and Saadat, M., "A new intelligent approach to patient-cooperative control of rehabilitation robots", ***International Journal of Engineering-Transactions C: Aspects***, Vol. 27, No. 3, (2013), 467-475.
12. Safartoobi, M., Dardel, M., Ghasemi, M. and MOHAMMADI, D.H., "Stabilization and walking control for a simple passive walker using computed torque method", ***International Journal of Engineering, Transactions B: Applications***, Vol. 27, No. 11, (2014), 1777-1786.
13. Liang, Q. and Wang, Y., "Flexible ankle based on pkm with force/torque sensor for humanoid robot", ***International Journal of Engineering, Transactions B: Applications***, Vol. 24, No. 4, (2011), 377-385.
14. Davis RB, O.S., DeLuca PA, Romness MJ, "Clinical gait analysis and its role in treatment decision-making", ***Medscape Orthopaedics & Sports Medicine eJournal***, Vol. 2, No. 5, (1998).
15. Perry, J., "Gait analysis—normal and pathological gait", ***Slack Incorporated, USA***, (1992), 54-62.
16. Zoss, A. and Kazerooni, H., "Design of an electrically actuated lower extremity exoskeleton", ***Advanced Robotics***, Vol. 20, No. 9, (2006), 967-988.
17. Zinn, M., Khatib, O., Roth, B. and Salisbury, J.K., "Towards a human-centered intrinsically safe robotic manipulator", in IARPIEEE/RAS joint workshop on technical challenges for dependable robots in human environments, Toulouse, France., (2002).
18. Hogan, N., "Impedance control: An approach to manipulation: Part iii applications", ***Journal of dynamic systems, measurement, and control***, Vol. 107, No. 2, (1985), 17-25.
19. Whitney, D.E., "Force feedback control of manipulator fine motions", ***Productivity***, (1976), 687-693.
20. Chiaverini, S., Siciliano, B. and Villani, L., "A survey of robot interaction control schemes with experimental comparison", ***Mechatronics, IEEE/ASME Transactions On***, Vol. 4, No. 3, (1999), 273-285.
21. Lam, T., Anderschitz, M. and Dietz, V., "Contribution of feedback and feedforward strategies to locomotor adaptations", ***Journal of neurophysiology***, Vol. 95, No. 2, (2006), 766-773.
22. Reinkensmeyer, D., Aoyagi, D., Emken, J., Galvez, J., Ichinose, W., Kerdanyan, G., Nessler, J., Maneekobkunwong, S., Timoszyk, B. and Vallance, K., "Robotic gait training: Toward more natural movements and optimal training algorithms", in Conf Proc IEEE Eng Med Biol Soc., (2004), 4818-4821.
23. Winter, D.A., "Biomechanics and motor control of human movement, Wiley, (2009).

Effect of Target Impedance Selection on the Lower Extremity Assistive Exoskeleton Performance

A. Taherifar[a], A. Selk Ghafari[b], G. Vossoughi[a]

[a] *School of Mechanical Engineering, Sharif University of Technology, Tehran, Iran*
[b] *School of Science and Engineering, Sharif University of Technology, International Campus, Kish Island, Iran*

PAPER INFO

Paper history:
Received 09 December 2015
Received in revised form 31 January 2016
Accepted 02 June 2016

Keywords:
Lower Limb Exoskeleton
Impedance Control
Human-robot Modelling
Interaction Modelling

چکیده

ربات های افزایش توان کاربرد گسترده ای در توانبخشی رباتیکی و افزایش توان کاربر دارند. یکی از روشهای کنترلی متداول مورد استفاده در این رباتها کنترلرامپدانسی می باشد. کنترل امپدانس امکان ایجاد تمرینات توانبخشی متنوع، با تغییر امپدانس هدف را میسر میسازد. یکی از روشهای متداول تعیین ضرایب امپدانسی که در تحقیقات صورت گرفته به آن اشاره شده است تعیین امپدانس هدف به روش تجربی و بر پایه سعی و خطا میباشد. در تحقیق حاضر، با ارائه یک چهارچوب عمومی امکان بررسی تاثیر امپدانس هدف بر روی عملکرد ربات های افزایش توان و نیز الگوی حرکتی انسان مورد مطالعه قرار میگیرد. در این مقاله، مدل دینامیکی صفحه ای حاکم بر انسان–ربات افزایش توان استخراج شده و برای شبیه سازی راه رفتن مورد استفاده قرار میگیرد. همچنین مدل جدیدی برای تعامل انسان و ربات افزایش توان معرفی میگردد. نتایج حاصل از شبیه سازی دینامیکی سیستم مورد مطالعه، امکان بررسی تاثیر نحوه تعیین ضرایب امپدانس هدف با کمینه کردن معیارهای مختلفی نظیر میزان مصرف انرژی، نیروی تعاملی بین ربات و انسان و نیز خطای ردیابی موقعیت را فراهم میسازد. در نتیجه روش ارائه شده در این مقاله میتواند بعنوان یکی از راهکارهای مناسب برای انتخاب موثر پارامترهای امپدانسی در رباتهای توان دهی مورد استفاده قرار گیرد.

***doi**: 10.5829/idosi.ije.2016.29.06c.00*